McDaniel, C. L. (1972). *J. Am. Ceram. Soc.* **55**, 426–427.
Maeda, H., Tanaka, Y., Fukutomi, M. & Asano, T. (1988). *Jpn J. Appl. Phys.* **27**, L209.
Michel, C., Hervieu, M., Borel, M. M., Grandin, A., Deslandes, F., Provost, J. & Raveau, B. (1987). *Z. Phys.* **B68**, 421–424.
Ohsato, H., Sugimura, T. & Kageyama, K. (1981). *J. Cryst. Growth*, **51**, 1–5.
Randall, J. J. & Katz, L. (1959). *Acta Cryst.* **12**, 519–521.
Randall, J. J. & Ward, R. (1969). *J. Am. Chem. Soc.* **81**, 2629–2631.
Roth, R. S., Rawn, C. J. & Bendersky, L. A. (1990). *J. Mater. Res.* **5** (1), 46–52.
Roth, R. S., Rawn, C. J., Burton, B. P. & Beech, F. (1990*a*). *J. Res. NIST*, March–April.
Roth, R. S., Rawn, C. J., Burton, B. P. & Beech, F. (1990*b*). *J. Res. NIST*, May–June.
Saggio, J. A., Sujata, K., Hahn, J., Hwu, S. J., Poeppelmeier, K. R. & Mason, T. O. (1989). *J. Am. Ceram. Soc.* **72**(5), 849–853.
Schneider, S. J. & McDaniel, C. L. (1969). *J. Am. Ceram. Soc.* **52**(9), 518–519.
Schwartz, K. B., Parise, J. B., Prewitt, C. T. & Shannon, R. D. (1982). *Acta Cryst.* B**38**, 2109–2116.
Schwartz, K. B., Parise, J. B., Prewitt, C. T. & Shannon, R. D. (1983). *Acta Cryst.* B**39**, 217–226.
Schwartz, K. B. & Prewitt, C. T. (1984). *J. Phys. Chem. Solids*, **45**(1), 1–21, and references therein.
Schwartz, K. B., Prewitt, C. T., Shannon, R. D., Corliss, L. M., Hastings, J. M. & Chamberland, B. L. (1982). *Acta Cryst.* B**38**, 363–368.
Strobel, P., Kelleher, K., Holtzberg, F. & Worthington, T. (1988). *Physica*, C**156**, 343–440.
Tu, H. Y., Hodeau, J. L., Bordet, P., Chandrashekhar, G. V., Fournier, T., Strobel, P. & Marezio, M. (1990). *Acta Cryst.* A**46**, C-336.
Wilkinson, A. P. & Cheetham, A. K. (1989). *Acta Cryst.* C**45**, 1672–1674.
Wilkinson, A. P., Cheetham, A. K., Kunnmann, W. & Kvick, A. (1991). In the press.

Acta Cryst. (1992). B**48**, 11–16

Structure Refinement of Al_3Zr using Single-Crystal X-ray Diffraction, Powder Neutron Diffraction and CBED

By Y. Ma

Department of Physics, University of Oslo, 1048 *Blindern*, 0316 *Oslo* 3, *Norway*

C. Rømming

Department of Chemistry, University of Oslo, 1033 *Blindern*, 0315 *Oslo* 3, *Norway*

B. Lebech

Risø National Laboratory, DK-4000 *Roskilde, Denmark*

and J. Gjønnes and J. Taftø

Department of Physics, University of Oslo, 1048 *Blindern*, 0316 *Oslo* 3, *Norway*

(*Received* 27 *June* 1991; *accepted* 2 *September* 1991)

Abstract

The structure of the intermetallic compound Al_3Zr has been studied at 293 K by single-crystal X-ray diffraction (Mo $K\alpha$ radiation, $\lambda = 0.71069$ Å), powder neutron diffraction {λ[Ge(711)] = 1.0867 Å} and convergent-beam electron diffraction (CBED) (200 keV, $\lambda = 0.0251$ Å). The structure of Al_3Zr comprises four close-packed metal sub-lattices and has the tetragonal space group *I*4/*mmm* with $a = 3.9993\ (5)$, $c = 17.283\ (2)$ Å, $V = 276.43\ (6)$ Å^3, $Z = 4$, $D_x = 4.136$ g cm^{-3}, $\mu = 45.11$ cm^{-1}. The new z coordinates of four Al and four Zr atoms on the e position [$z_{Al(e)}$ and $z_{Zr(e)}$] were determined by single-crystal X-ray diffraction: $z_{Al(e)} = 0.37498\ (5)$ and $z_{Zr(e)} = 0.11886\ (1)$. The results from single-crystal X-ray diffraction were confirmed by powder neutron diffraction, although they differ considerably from previously reported data [Brauer (1939). *Z. Anorg. Chem.* **242**, 1–22] and differ in parts from the CBED work. The structure was refined to $R = 0.016$, $wR = 0.021$ for 304 unique observed reflections for single-crystal X-ray diffraction, while it was refined to $R = 0.064$, $wR = 0.095$ for 43 resolved peaks for powder neutron diffraction. A large anisotropic effect for the temperature factor of the Al atoms on the e position [Al(e)] was found by single-crystal X-ray diffraction, which may have both thermal and non-thermal origins. For the newly proposed CBED technique, a wide cone of incident rays was used to obtain inten-

0108-7681/92/010011-06$03.00

sity data from high reflections (0,0,32–0,0,72) of the 00*l* systematic row. These high-angle reflection intensities were interpreted kinematically and used for the refinement of the *z* coordinate along the systematic row. The *z* coordinate of the Zr(*e*) atom refined by CBED is consistent with that obtained by single-crystal X-ray diffraction, while a considerable discrepancy between the two techniques exists for the *z* coordinate of Al(*e*). This is an indication of both promising features and limitations of the technique.

Introduction

Intermetallic trialuminides Al_3X with the refractory metals Ti, Zr *etc.* are of potential interest as structural materials owing to their low densities, high oxidation resistance and high melting points. The main limitation is their extreme brittleness, which has been discussed in relation to the crystal structures (Fu, 1990; George, Horton, Porter & Schneibel, 1990; Hong & Freeman, 1990). These are quite simple structures, based on ordering of close-packed metal sub-lattices, *e.g.* the cubic $L1_2$, the tetragonal $D0_{22}$ or $D0_{23}$ and the hexagonal $D0_{19}$ structures. The tetragonal cells may have appreciable tetragonal deformation of the basic $L1_2$ subcell. However, crystal structure determinations of these materials are mostly quite old (Brauer, 1939; Black, 1955). During a study of an Al–Zr alloy containing μm-size precipitates of Al_3Zr using convergent-beam electron diffraction (CBED), large discrepancies in the refined *z* coordinates of the Zr(*e*) and Al(*e*) atoms were found between previous powder X-ray diffraction (Brauer, 1939) and a recently proposed electron diffraction method, CBED, with large Bragg and convergent angles (Taftø & Metzger, 1985; Tomokiyo & Kuroiwa, 1991). Since the technique has only recently been developed, it was therefore decided to carry out a coordinate refinement of Al_3Zr using established quantitative methods of single-crystal X-ray diffraction and powder neutron diffraction. Accurate structural data are also of great importance in efforts to understand the structural transformation caused by macroalloying with small amounts of a third element in these types of intermetallics. The newly refined coordinates differ appreciably from the data of previous powder X-ray diffraction and we present here the main results from the single-crystal X-ray, powder neutron and convergent-beam electron diffraction studies.

Experimental

Sample preparation

The samples were prepared from an Al–Zr ingot with 5.4% wt Zr, supplied by Hydro Aluminium AS, Sunndal Verk, Norway. The ingot contained a dispersion of small Al_3Zr particles, typically 1–50 μm in diameter, within the aluminium grains (Fig. 1*a*). As these were too small for single-crystal X-ray diffraction, the ingot was remelted at about 1273 K in an electric powered furnace under vacuum and kept for about 100 h at this temperature, *i.e.* above the melting point of Al, but well below that of the aluminide (1853 K). The Al_3Zr particles coarsened and sank to the bottom of the crucible owing to their higher density. Particles with diameters up to 5 mm were formed in this way (Fig. 1*b*).

In order to extract the Al_3Zr particles out of the Al matrix, an electrolytic method (Raynor & Wakeman, 1946) was adopted. The Al–Zr ingot was arranged as the anode of an electrolytic cell with an Ni strip as its cathode and the electrolyte was made of dilute hydrochloric and nitric acids with an H_2O:HCl:-HNO_3 ratio of 100:1:1. The potential difference between the anode and cathode was 9 V. The Al matrix was slowly dissolved away, while H_2 gas was generated on the Ni cathode. The Al_3Zr particles with their strong oxidation resistance remained as residues and gradually fell into a small container at

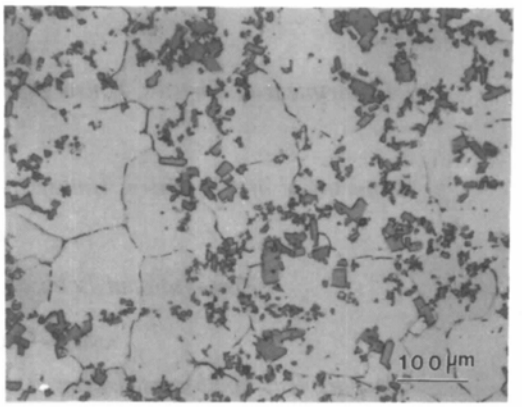

(*a*)

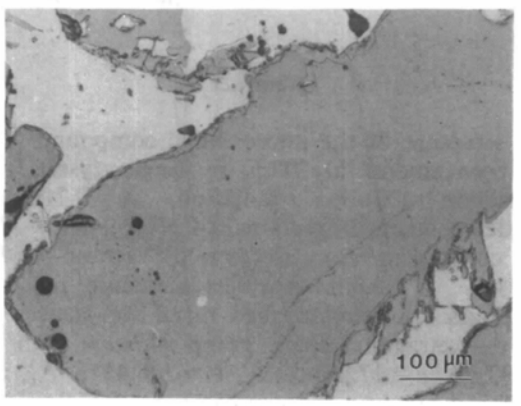

(*b*)

Fig. 1. Photomicrographs of the Al–Zr alloy with Al_3Zr particles in the Al matrix (*a*) before the heat treatment and (*b*) after the heat treatment. The magnification of both is × 160.

the bottom of the large container. The collected residues were then washed thoroughly with 50% nitric acid, followed by repeated washing with water. After rinsing with alcohol, the residues were dried by gentle heating. One of these particles was examined by scanning electron microscopy (SEM) as shown in Fig. 2, which clearly indicates the anisotropic nature of the growth. The shorter dimension was along the c axis as checked by the electron channelling method. The data from EDS after a bulk absorption correction had been applied showed that the compound contains $74.15 \pm 1\%$ Al and $25.85 \pm 1\%$ Zr. We therefore concluded that it was a stoichiometric compound. The size of the selected crystal was about 200 μm. To introduce some defects and form an ideally imperfect crystal in order to avoid multiple scattering in single-crystal X-ray diffraction, the selected crystal was quenched from room temperature to liquid nitrogen temperature about ten times. For the powder neutron diffraction, the small Al_3Zr particles were extracted directly from the Al–Zr ingot and the rest of the treatment was the same as described above.

Single-crystal X-ray diffraction refinement of Al_3Zr

The basic crystal structure of Al_3Zr is tetragonal, $I4/mmm$, with atoms at the special positions c, d and e (Fig. 3). There are two positional parameters for the four Al and four Zr atoms on the e position for further refinement. These two parameters were previously refined by Brauer using X-ray powder diffraction in 1939, which gave the following results: $z_{Al(e)} = 0.361$ and $z_{Zr(e)} = 0.122$ with lattice parameters of $a = 4.014$ and $c = 17.320$ Å.

For single-crystal X-ray diffraction, the intensities were measured with a Nicolet $P3/F$ diffractometer using graphite-monochromatized Mo $K\alpha$ radiation. The lattice parameters were determined from 25 reflections with $32 < 2\theta < 43°$. The intensities were measured by the ω–2θ technique with a scan speed of $2.0°\ \text{min}^{-1}$ (2θ) and the scan range was from 1.2° below $2\theta(\alpha_1)$ to 1.6° above $2\theta(\alpha_2)$. Three standard reflections were monitored for every 135 intensity measurements without significant variation. The size of the crystal was $220 \times 180 \times 90$ μm and data were collected at 293 K from a hemisphere of reciprocal space within $\sin\theta/\lambda_{max} = 0.9$ Å^{-1} for $0 \le h \le 7$, $-7 \le k \le 7$ and $-31 \le l \le 31$. 1603 observed reflections [$I > 3\sigma(I)$] merged to 304 unique reflections with $R_{int} = 0.023$, where σ is defined as $\sigma^2(I) = P + B + [0.025(P - B)]^2$, P = scan counts and B = background counts. The data were corrected for Lorentz, polarization and absorption effects [empirical absorption correction (Walker & Stuart, 1983); minimum and maximum absorption corrections were 0.883 and 1.219, respectively]. The *GX* package (Mallinson & Muir, 1985) was used for all calculations. Starting coordinates in a full-matrix least-squares refinement on F [$w = 1/\sigma^2(F)$] were those given by Brauer (1939) and all atoms were refined anisotropically. The total number of refined parameters was 13 and the over-determination ratio was 23. For the final refinement $R = 0.016$, $wR = 0.021$, $S = 3.58$, $(\Delta/\sigma) < 0.05$ and $\Delta\rho_{max} = 0.74$ e Å^{-3}. Scattering factors were taken from *International Tables for X-ray Crystallography* (1974, Vol. IV, Table 2.2B, pp. 99, 101). The final results are listed in Table 1.*

Powder neutron diffraction refinement of Al_3Zr

The powder neutron diffraction refinement was carried out at Risø National Laboratory, Denmark, for several reasons. (*a*) There were considerable dis-

* Lists of structure factors, and observed and calculated intensities *versus* scanning angle have been deposited with the British Library Document Supply Centre as Supplementary Publication No. SUP 54564 (19 pp.). Copies may be obtained through The Technical Editor, International Union of Crystallography, 5 Abbey Square, Chester CH1 2HU, England. [CIF reference: AB0236]

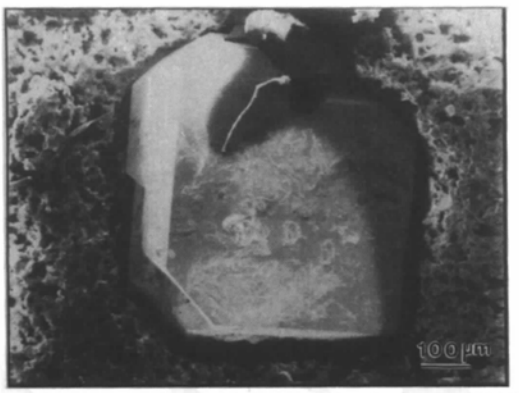

Fig. 2. SEM image of one Al_3Zr particle after about 100 h of crystal growth. The magnification is × 100.

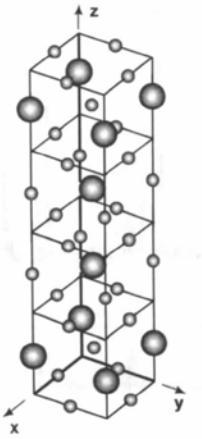

Fig. 3. Schematic diagram of one unit cell of Al_3Zr. The large dots denote Zr, while the small ones denote Al.

Table 1. *Atomic coordinates and thermal parameters*

Al_3Zr (single-crystal X-ray) tetragonal, *I4/mmm*, $a = 3.9993$ and $c = 17.283$ Å.

	x	y	z	U_{11}	U_{22}	U_{33}	B_{eq} (Å^2)	R
Old powder X-ray								
Al(*c*)	0	0.5	0					
Al(*d*)	0	0.5	0.25					
Al(*e*)	0	0	0.361					
Zr(*e*)	0	0	0.122					
Single-crystal X-ray								
Al(*c*)	0	0.5	0	0.0083 (3)	0.0055 (3)	0.0063 (3)	0.53 (2)	
Al(*d*)	0	0.5	0.25	0.0077 (2)	0.0077	0.0072 (3)	0.59 (2)	
Al(*e*)	0	0	0.37498 (5)	0.0059 (2)	0.0059	0.0131 (3)	0.66 (2)	0.016
Zr(*e*)	0	0	0.11886 (1)	0.0047 (1)	0.0047	0.0045 (1)	0.36 (1)	
Powder neutron								
Al(*c*)	0	0.5	0				0.3 (1)	
Al(*d*)	0	0.5	0.25				0.3 (1)	
Al(*e*)	0	0	0.3751 (6)				0.5 (1)	0.064
Zr(*e*)	0	0	0.1191 (2)				0.4 (1)	
							$B_{eq}(z)$ (Å^2)	
CBED								
Al(*c*)	0	0.5	0				0.2 (1)	
Al(*d*)	0	0.5	0.25				0.2 (1)	
Al(*e*)	0	0	0.3670 (5)				0.4 (1)	0.08
Zr(*e*)	0	0	0.1190 (5)				0.6 (1)	

crepancies between the results of the single-crystal X-ray diffraction and those of older powder X-ray diffraction and also the current electron diffraction work. (*b*) The z coordinate of Al(*e*), for which there are particularly large discrepancies among the results of the above three methods, can be more reliably refined with neutron rather than with X-ray or electron diffraction because the relative scattering strength of Al to neutrons ($b_{Al}/b_{Zr} \simeq 0.5$, b denotes scattering length) is stronger than that to X-rays or electrons ($f_{Al}/f_{Zr} \simeq 0.3$, f denotes atomic scattering factor). (*c*) The temperature-factor analysis is not influenced by absorption and form-factor effects. (*d*) Surface effects, which play an unknown role, are negligible in powder neutron diffraction. The experiments were carried out at the high-resolution multidetector powder neutron diffractometer with reactor DR3 at Risø National Laboratory. The Al_3Zr powder sample was made directly from an Al–Zr ingot as previously described and the incident neutron radiation of wavelength 1.0867 Å from a vertically focusing Ge(711) monochromator at a take-off angle of 85° was used. A total of 43 reflection peaks were resolved and the data were evaluated using the *EDINP* powder refinement program (Pawley, 1980). The peaks were fitted with a Gaussian function. The variation of width with scattering angle 2θ is described by the following formula: $\Delta(2\theta)^2 = U\tan^2\theta + V\tan\theta T + W$, where U, V and W are three refinable peak-shape parameters. Asymmetry effects were not taken into account, which was responsible for the relatively high reading for low-angle peaks in the difference plot. The background was fitted by linearly connecting 21 sampling points in the background of the powder neutron diffraction pattern within $10 \le 2\theta \le 110°$ and an additional constant background parameter was refinable. The refinements were carried out with isotropic temperature factors and the range over which contributions from resolved reflections were considered was $8.0 \le 2\theta \le 113.5°$. The experimental and calculated patterns and their difference plot are shown in Fig. 4 and the final refined results are listed in Table 1.*

* See deposition footnote.

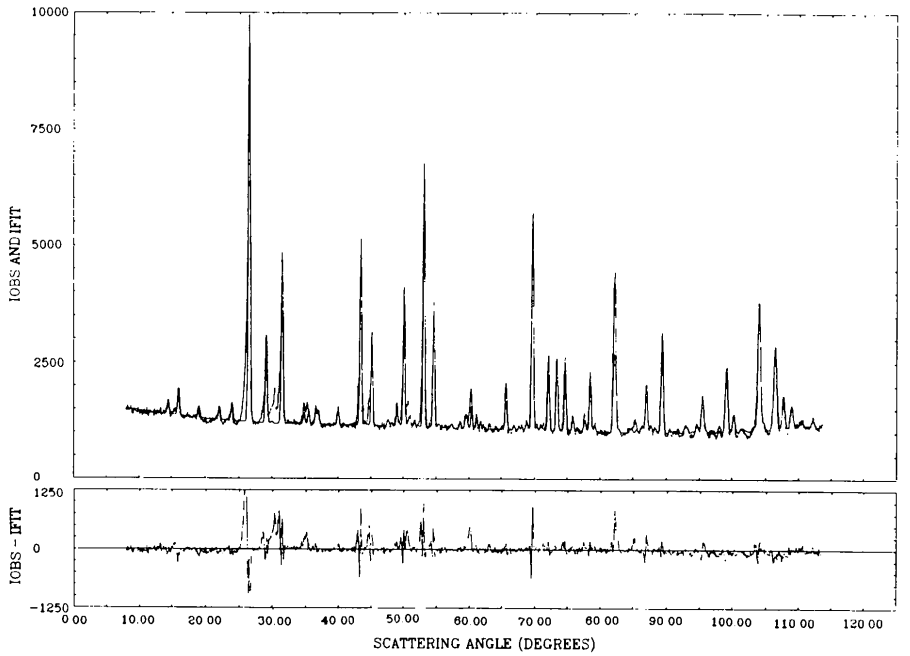

Fig. 4. Observed and calculated powder neutron diffraction patterns from Al_3Zr and the difference plot.

Convergent-beam electron diffraction (CBED) refinement

The present CBED technique used for structure refinement was first developed by Taftø & Metzger (1985), who showed that a wide cone of incident rays for a converged electron beam in an electron microscope could be used to obtain intensity data from many high-order reflections of a systematic row. Later it was applied to α-Al_2O_3 with one undetermined displacement parameter of Al atoms on octahedra sites formed by O atoms (Tomokiyo & Kuroiwa, 1991). The robust feature of the technique is due to the fact that it is possible to use quasi-kinematical arguments to interpret the intensities of high-order reflections (Tomokiyo & Kuroiwa, 1991) because the extinction distance ξ_g for g far out of reciprocal space is much larger than the thickness of a conventional transmission electron microscopy (TEM) specimen, *i.e.* $I_g \propto |F_g|^2$, where I_g is the intensity of the reflection g and F_g is the structure factor for the reflection. The structure factor of Al_3Zr for the reflections along the systematic row $00l$ is $F_{00l} = 2[f_{Zr(e)}\cos(i2\pi z_{Zr(e)}l) + f_{Al(e)}\cos(i2\pi z_{Al(e)}l) + f_{Al(c)} + f_{Al(d)}\exp(i\pi l/2)][1 + \exp(i\pi l)]$ where f_{Zr} and f_{Al} are the atomic scattering factors of Zr and Al, respectively. Subscripts e, c and d denote special symmetrical positions of $I4/mmm$. The TEM specimen was made from the Al–Zr ingot after the heat treatment as previously described. It was thinned by metallurgical and jet polishing. The experiment was performed in a JEM 200CX electron microscope with 200 keV accelerating energy, at the University of Oslo, Norway. Fig. 5 shows one of the CBED patterns taken with large Bragg and convergent angles in order to measure intensities of $00l$ reflections for high l values. From the densitometric recordings of the CBED patterns intensities for $l = 32$–72 were obtained. The background was fitted with a cubic spline. The refinement involved five parameters: $z_{Zr(e)}$, $B_{Zr(e)}$, $z_{Al(e)}$, $B_{Al(c,d)}$ and $B_{Al(e)}$, where B denotes temperature factors. The same thermal parameters were used for the Al atoms on the c and d positions [Al(c) and Al(d)]. The results are listed in Table 1. As can be seen, owing to the potential overlap of Al(e) and Zr(e) along the z axis, only the z coordinate of Zr(e) can be determined with reasonable accuracy from these data.

Discussion

The results of the four different techniques listed in Table 1 show that discrepancies between them for the z coordinate of Zr(e) (0.002–0.05 Å) are much smaller than those for Al(e) (0.002–0.24 Å). This is because structure factors are usually dominated by heavy atoms and the displacements of heavy atoms in a structure can be more reliably refined by various refinement techniques, compared with those of light atoms. Although the single-crystal X-ray results differ markedly from the previous reported data, they are confirmed by the data of powder neutron diffraction. The differences between the results of the two techniques are $\Delta z_{Zr(e)} = z_{Zr(e)}(N) - z_{Zr(e)}(X) = 0.1191 - 0.11886 = 0.00024$ and $\Delta z_{Al(e)} = z_{Al(e)}(N) - z_{Al(e)}(X) = 0.3751 - 0.37498 = 0.00012$. They are well within the uncertainty range of neutron diffraction. In addition, the single-crystal X-ray results also have a very satisfactory R value, which is a key indication of the refinement reliability. In other words, the results from the single-crystal X-ray diffraction of Al_3Zr should be taken as the new precise and reliable structure data for this material.

A remarkable feature of the single-crystal X-ray results is the rather large anisotropic effects of the temperature factors for the Al(e) atom: U_{33}/U_{11}, $U_{33}/U_{22} = 2.22$. The thermal origin of this anisotropic effect is quite clear. For Al(e), the near-neighbour distances in the xy plane are $d_{Al—Al} = 3.9993$ and $d_{Al—Zr} = 2.8299$ Å (see Fig. 3), while the near-neighbour distances along the z axis are $d_{Al—Zr} = 4.4265$ and $d_{Al—Al} = 4.321$ Å (see Fig. 3). This means that the spacing of thermal vibration for Al(e) along the z axis is larger than that in the xy plane, which is mainly responsible for its anisotropic temperature factor. On the other hand, this large anisotropic effect may also have some non-thermal origin, possibly related to defects, such as stacking faults along the z axis. Extensive diffuse scattering observed in some projections in electron diffraction appears to support this. The directional bonding effects along the z axis for the Al(e) atom (both Al—Al and Al—Zr bonds), which are considered to be responsible for the brittleness of this type of intermetallic, may also manifest themselves in this anisotropic temperature factor.

As Table 1 shows, the coordinate of Zr(e), $z_{Zr(e)}$, obtained from the CBED refinement is consistent

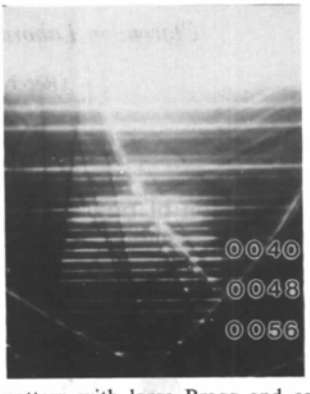

Fig. 5. CBED pattern with large Bragg and convergent angles from one Al_3Zr particle in the Al matrix. 17 reflections were recorded in one exposure.

with the data obtained from the single-crystal X-ray and powder neutron diffraction refinements, while the coordinate of Al(*e*), $z_{Al(e)}$, was poorly determined by the 00*l* electron data. This is mainly due to the fact that the heavy Zr(*e*) atom masked the Al(*e*) atom, which smeared out along the *z* axis because of its anisotropically large temperature factor found by single-crystal X-ray diffraction. Although this indicates the limitation of the CBED technique, it should be pointed out that a kinematic interpretation on high-order systematic reflections recorded in a CBED disc with large Bragg and convergent angles is feasible and as a simple technique it can be applied to μm-sized crystals in TEM experiments. It will also be promising to apply the technique to thermal or mechanical *in situ* observations in an electron microscope, at least for a quick semi-quantitative estimation on atomic structure variations of a μm-sized crystal. A detailed discussion of the technique based upon the data obtained from Al_3Zr will be presented elsewhere.

The differences between the temperature factors refined by single-crystal X-ray diffraction and powder neutron diffraction can be explained by several facts. Firstly, the anisotropic thermal effects were not taken into account in the powder neutron diffraction refinement, while the data from single-crystal X-ray diffraction results show that the Al(*e*) atom has significant anisotropic thermal behaviour. However, the neutron data confirm that Al(*e*) thermally vibrates more than Al(*c*) and Al(*d*). Secondly, various errors usually manifest themselves in the temperature factors and, lastly, the thermal histories of the samples for the two techniques are different and the powder sample for the neutron diffraction may have been more disordered.

This work was supported by the Norwegian Research Council for Science and the Humanities. The authors also would like to thank Hydro Aluminium Co. for supplying the ingot of Al–Zr alloy.

References

BLACK, P. J. (1955). *Acta Cryst.* **8**, 43–48.
BRAUER, G. (1939). *Z. Anorg. Chem.* **242**, 1–22.
FU, C. L. (1990). *J. Mater. Res.* **5**, 971–979.
GEORGE, E. P., HORTON, J. A., PORTER, W. D. & SCHNEIBEL, J. H. (1990). *J. Mater. Res.* **5**, 1639–1648.
HONG, T. & FREEMAN, A. J. (1990). *J. Mater. Res.* **6**, 330–338.
MALLINSON, P. R. & MUIR, K. W. (1985). *J. Appl. Cryst.* **18**, 51–53.
PAWLEY, G. S. (1980). *J. Appl. Cryst.* **13**, 630–633.
RAYNOR, G. V. & WAKEMAN, D. W. (1946). *Proc. R. Soc. London Ser. A*, **190**, 82–101.
TAFTØ, J. & METZGER, T. H. (1985). *J. Appl. Cryst.* **18**, 110–113.
TOMOKIYO, Y. & KUROIWA, T. (1991). *Proceedings of the XIIth International Congress for Electron Microscopy*, Vol. 2, pp. 526–527. San Francisco: San Francisco Press.
WALKER, N. & STUART, D. (1983). *Acta Cryst.* A**39**, 158–166.

Acta Cryst. (1992). B**48**, 16–21

Absolute Optical Chirality of Ammonium Dihydrogen Phosphate

BY K. STADNICKA AND A. MADEJ

Faculty of Chemistry, Jagiellonian University, Karasia 3, 30-060 *Kraków, Poland*

AND I. J. TEBBUTT AND A. M. GLAZER

*Clarendon Laboratory, Parks Road, Oxford OX*1 3*PU, England*

(*Received* 23 *May* 1991; *accepted* 4 *October* 1991)

Abstract

A theoretical prediction of optical rotation is made for the non-enantiomorphous material ammonium dihydrogen phosphate (ADP), based entirely on the known crystal structure. It is predicted that the (100) section, with axes chosen according to Khan & Baur [*Acta Cryst.* (1973), B**29**, 2721–2726], should be optically laevorotatory. Measurement of this material's optical rotation is reported for the first time using a specially constructed polarimeter. Together with X-ray Bijvoet-pair measurements, it has been possible to determine the *absolute optical chirality*, with the result that in the (100) section $\rho = -6.8\ (5)^\circ\ mm^{-1}$ (laevo) and in the (010) section $\rho = +6.8\ (5)^\circ\ mm^{-1}$ (dextro) for a wavelength $\lambda = 589.3$ nm.

Introduction

Ammonium dihydrogen phosphate (ADP) crystallizes in the non-enantiomorphic non-polar space

0108-7681/92/010016-06$03.00